

SCFlow: Optical Flow Estimation for Spiking Camera

Liwen Hu^{1,2*}, Rui Zhao^{1*}, Ziluo Ding¹, Ruiqin Xiong¹, Lei Ma^{1,2†}, Tiejun Huang^{1,2}

¹National Engineering Laboratory for Video Technology, Peking University

²Beijing Academy of Artificial Intelligence

{huliwen, ziluo, rxiong, lei.ma, tjhuang}@pku.edu.cn, ruizhao@stu.pku.edu.cn

Abstract

As a bio-inspired sensor with high temporal resolution, Spiking camera has an enormous potential in real applications, especially for motion estimation in high-speed scenes. Optical flow estimation has achieved remarkable success in image-based and event-based vision, but conventional optical flow algorithms are not well matched to the spike stream data. This paper presents, SCFlow, a novel deep learning pipeline for optical flow estimation for spiking camera. Importantly, we introduce an proper input representation of a given spike stream, which is fed into SCFlow as the sole input. We introduce the *first* spiking camera simulator (SPCS). Furthermore, based on SPCS, we first propose two optical flow datasets for spiking camera (SPIKingly Flying Things and Photo-realistic High-speed Motion, denoted as SPIFT and PHM respectively) corresponding to random high-speed and well-designed scenes. Empirically, we show that the SCFlow can predict optical flow from spike stream in different high-speed scenes, and express superiority to existing methods on the datasets. *All codes and constructed datasets will be released after publication.*

Introduction

Optical flow estimation has always been a popular topic in computer vision and applied on a wide range of applications, such as object segmentation (Bideau et al. 2018), video enhancement (Wang et al. 2020), and action recognition (Tu et al. 2019). However, the breakthrough of this field in high-speed scenes is impeded by blurred images, as fig.1(b), sampled by traditional cameras with low frame rate. To address the problems in high-speed scenes, some work raise the interest in event cameras (Patrick, Christoph, and Tobi 2008; Tobi and Bernabe 2010; Christian and Raphael 2014; Christoph, Daniel, and Rainer 2008; Guo, Huang, and Chen 2017) and attempt to estimate optical flow from the event stream (Zhu et al. 2018a, 2019a; Lee et al. 2020). Although event cameras with high temporal resolution can prevent the motion blur, the event stream that only encodes the change of luminance intensity might be insufficient for optical flow estimation in all regions, especially for some less-texture scenes.

*These authors contributed equally.

†Corresponding author.

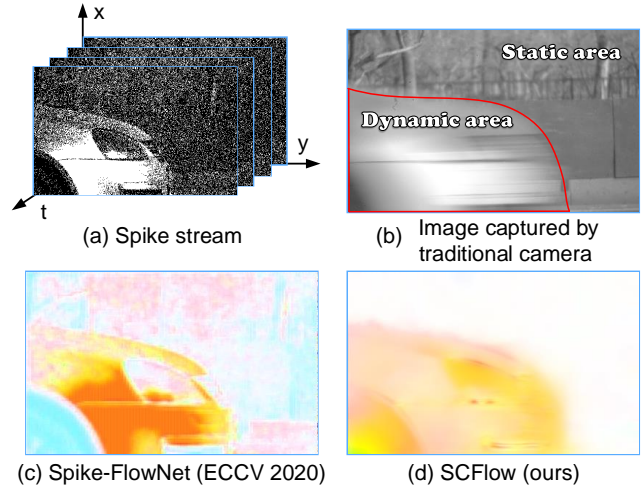


Figure 1: The optical flow estimation for a car traveling at a speed of 100 km/h. (a) **Real** spike stream captured by the spiking camera. (b) The image captured by tradition camera where a car moves in a straight line and no movement in the background. (c-d) the estimated optical flows with different method. Our proposed method has convincing results, distinguish dynamic area and static area.

Different from event cameras, spiking camera (Dong et al. 2017; Zhu et al. 2019b) can report per-pixel luminance intensity accumulation by firing spikes asynchronously. At each timestamp, when luminance intensity accumulation in a pixel exceeds the predefined threshold, a spike is sent and the accumulation is reset for that pixel, otherwise there is no spike at that position. Hence, instead of a grayscale image, the output of all pixels forms a binary matrix representing the presence of the spikes, also known as spike frame, and spike frames from all timestamps form the spike stream. Benefiting from the novel sampling mechanism, spiking camera not only has a high temporal resolution of 40000Hz, but also records the texture details of objects (Zhu et al. 2019b, 2020; Zheng et al. 2021; Zhao et al. 2021). Therefore, spiking camera that can clearly record high-speed scene information has an enormous potential for visual tasks in high-speed scene. However, there is no in-

investigation about spike-based optical flow estimation in the computer vision community yet. Besides, due to the difference in data representation, it is inappropriate to apply frame-based or event-based methods directly to spike frames (as fig.1(c)).

In this paper, we propose a novel neural network architecture, SCFlow, to estimate the optical flow from spike stream. First, the spikes in temporal windows are generally used as features for all pixels (Zhao et al. 2021). However, the temporal windows should be carefully chosen at each pixel due to the potential light change and object movement. Thus, we introduce a novel input representation of spike stream which allows temporal windows to be adaptively selected based on the motion prior. Then, for training our network, we first propose two spike-based optical flow datasets, SPIkingly Flying Things and Photo-realistic High-speed Motion, denoted as SPIFT and PHM respectively. SPIFT and PHM include 110 random scenes and 10 well-designed scenes respectively. Random scenes in SPIFT comprise random objects that translate and rotate in random background, like FlyingChairs (Dosovitskiy et al. 2015). Well-designed scenes in PHM are more lifelike and has a lot in common with the real world. Note that the datasets are generated by our proposed spiking camera simulator (SPCS). Empirically, we show that SCFlow can estimate optical flow well in high-speed scenes and achieve the state-of-the-art performance in comparison with existing image-based and event-based methods in our datasets.

In general, we attempt to exploit the potential of spiking camera in high-speed motion estimation and our main contributions are summarized as follows:

- 1) We propose the *first* spiking camera simulator (SPCS) which combines simulation function and rendering engine tightly. By using SPCS to render virtual scenes, the first spike-based optical flow datasets, SPIFT and PHM, is proposed.
- 2) We present SCFlow, the *first* deep learning architecture for optical flow estimation of spiking camera. Importantly, we introduce an novel input representation for a given spike stream allowing adaptive temporal window selection, which is fed into SCFlow as the sole input.
- 3) We train SCFlow on SPIFT dataset and estimate optical flow for spiking camera on PHM dataset. Experimental results demonstrates that our proposed SCFlow can estimate flow field from spike streams efficiently.

Related Work

Image-based and Event-based Optical Flow

Optical flow estimation for frame-based cameras has been a classical vision task since it was first introduced by Horn and Schunck (Horn and Schunck 1981). Early methods describe the essence of flow field via an illumination consistency assumption and combine it with a smoothness constraint to avoid the ill-posed condition. Many effective modules were introduced to subsequent algorithms such as estimating the flow fields coarse-to-fine via a pyramid structure and warping (Brox et al. 2004) and median filtering (Sun, Roth, and

Black 2010). However, these variational methods suffer a huge time cost. In the variational age, the datasets to evaluate an optical flow algorithm are mainly Middlebury (Baker et al. 2011), Sintel (Butler et al. 2012) and KITTI (Geiger, Lenz, and Urtasun 2012; Menze and Geiger 2015). The flow ground truth of Middlebury dataset is obtained via UV illumination or artificial synthesis, which has only dozens of samples. The Sintel dataset is derived from an open source 3D animated short film. The KITTI dataset gets flow ground truth with LIDAR, which causes the flow field to be sparse. However, these datasets are not adequate in quantitative terms for training a deep neural network.

Dosovitskiy et al. (Dosovitskiy et al. 2015) firstly propose a large dataset FlyingChairs to train an end-to-end neural network FlowNet via supervised learning. FlowNet 2.0 (Ilg et al. 2017) improves the performance by stacking the network, which makes the model too large. Knowledge from classical methods such as pyramid, warping (Brox et al. 2004) and cost volume (Scharstein and Szeliski 2002) was introduced to optical flow estimation network to make it compact (Sun et al. 2018). However, ground truth of optical flow is hard to obtain. Deep optical flow networks training by unsupervised scheme were proposed to handle this problem (Jason, Harley, and Derpanis 2016), similar with variational methods, it employ photometric loss and smoothness loss. To improve the reliability of supervision signal, bi-directional flow estimation (Meister, Hur, and Roth 2018) was proposed to detect occlusion area and stop its back-propagation. Recently, self-supervision methods (Liu et al. 2019, 2020) were proposed to improve the performance of unsupervised networks. Optical flow estimation for event camera has attracted more and more interest due to its high temporal resolution. The MVSEC (Zhu et al. 2018a) dataset gets flow ground truth through LIDAR and records natural scenes using event camera and gray camera simultaneously. EV-FlowNet (Zhu et al. 2018b) can be regarded as the first deep learning method for event-based optical flow, which is trained by photometric loss and smoothness loss with the help of gray images. Zhu et al. (Zhu et al. 2019a) train the network with a loss function designed to eliminate the motion blur in event spikes. SpikeFlowNet (Lee et al. 2020) propose a hybrid network with spiking neural network (SNN) encoder to better exploit the temporal information in event spikes. STEFlow (Ding et al. 2021) further improves the performance using recurrent neural networks as encoder.

Development of Spiking Camera

Spiking camera is a bio-inspired sensor with high temporal resolution. Different from event cameras, spiking camera (Dong et al. 2017; Zhu et al. 2019b) can report per-pixel luminance intensity accumulation by firing spikes asynchronously. Benefit from its distinct sampling mechanism, spiking camera can record all the texture details of objects *theoretically*. Given its huge potential in applications, especially for high-speed scenes, low-level vision tasks based on spiking camera have developed rapidly. (Zhu et al. 2019b) first provided high-speed imaging for spiking camera by counting the time interval (TFI) and the number of spikes (TFP). (Zhao, Xiong, and Huang 2020) im-

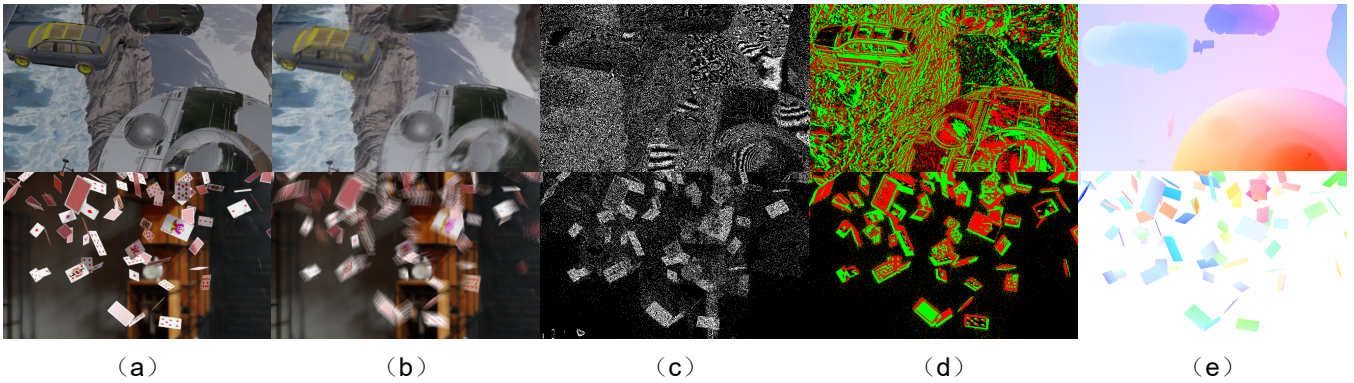


Figure 2: Two examples of the output of our simulator. The figures in first line correspond to training set and the figures in second line correspond to testing set. (a) High-speed sampling scene. (b) Image. (c) Spiking stream where white pixels correspond to spike and other pixels are encoded as black. (d) Event stream where “ON” events are encoded as red and “OFF” events are encoded as green. (e) Optical flow.

proved the smoothness of reconstructed images through motion aligned filtering. (Zhu et al. 2020; Zheng et al. 2021) and (Zhao et al. 2021) respectively use SNN and convolutional neural network to reconstruct high-speed images from spike stream, which greatly improved the reconstruction quality.

Preliminary

Spiking Camera Model

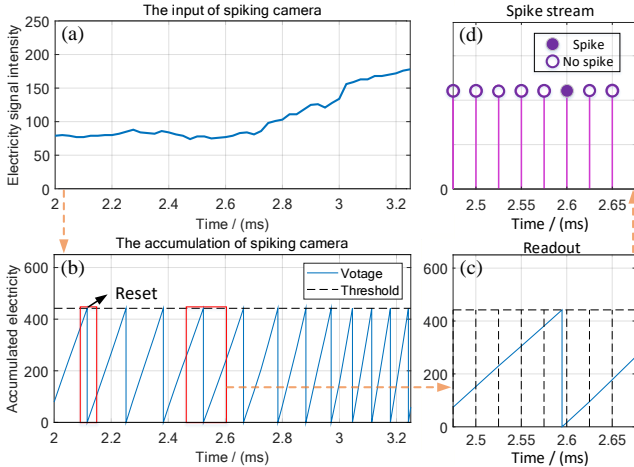


Figure 3: The illustration of spiking camera model. (a) the input electrical signal at a pixel. (b) the accumulation corresponding to the pixel. (c) the polling readout of spikes where the spiking camera checks for the generation of spike at a frequency of 40000 Hz. (d) Generated spike stream at the pixel.

Spiking camera mimicking the retina fovea consists of an $H \times W$ array of pixels and can report per-pixel luminance intensity accumulation by firing spikes asynchronously. Specifically, in spiking camera, the intensity of light is con-

verted into voltage by the photoreceptor. Once the analog-to-digital converter completes the signal conversion and outputs the digital brightness, the accumulator at each pixel accumulates the brightness. At time t , for pixel (i, j) , if the accumulated brightness arrives a fixed threshold ϕ (as (1)), then a spike is fired and the corresponding accumulator is reset (as fig.3).

$$\mathbf{A}(i, j, t) = \int_{t_{i,j}^{\text{pre}}}^t I(i, j, \tau) d\tau \geq \phi, \quad (1)$$

where $i, j \in \mathbb{Z}, i \leq H, j \leq W, k \leq N$, $A(i, j, t)$ is the accumulated brightness at time t , $I(i, j, \tau)$ refers to the brightness of pixel (i, j) at time τ , and $t_{i,j}^{\text{pre}}$ expresses the last time when a spike is fired at pixel (i, j) before time t . If t is the first time to send a spike, then $t_{i,j}^{\text{pre}}$ is set 0. In fact, due to the limitations of circuit technology, the spike reading times are quantified. Hence, asynchronous spikes are read out synchronously. Specifically, all pixels periodically check the spike flag at time $n\Delta t, n \in \mathbb{N}$, where Δt is a short interval of microseconds. Therefore, the output of all pixels forms a $H \times W$ binary spiking frame. As the time goes on, the camera would produce a sequence of spike frames, i.e., an $H \times W \times N$ binary spike stream and can be mathematically defined as,

$$\mathbf{S}(i, j, n\Delta t) = \begin{cases} 1 & \text{if } \exists t \in ((n-1)\Delta t, n\Delta t], \text{ s.t. } \mathbf{A}(i, j, t) \geq \phi, \\ 0 & \text{if } \forall t \in ((n-1)\Delta t, n\Delta t], \mathbf{A}(i, j, t) < \phi, \end{cases} \quad (2)$$

Accordingly, the average brightness of pixel (i, j) between times a and b can be evaluated by counting the number of spikes (Zhu et al. 2019b), i.e.,

$$\frac{\phi \sum_{a \leq n\Delta t \leq b} \mathbf{S}(i, j, n\Delta t)}{b - a} \quad (3)$$

Optical Flow for Spiking Camera

Problem Statement We use $S_n \in \{0, 1\}^{W \times H}$ to denote the n -th spike frame and F_{t_i, t_j} to denote optical flow be-

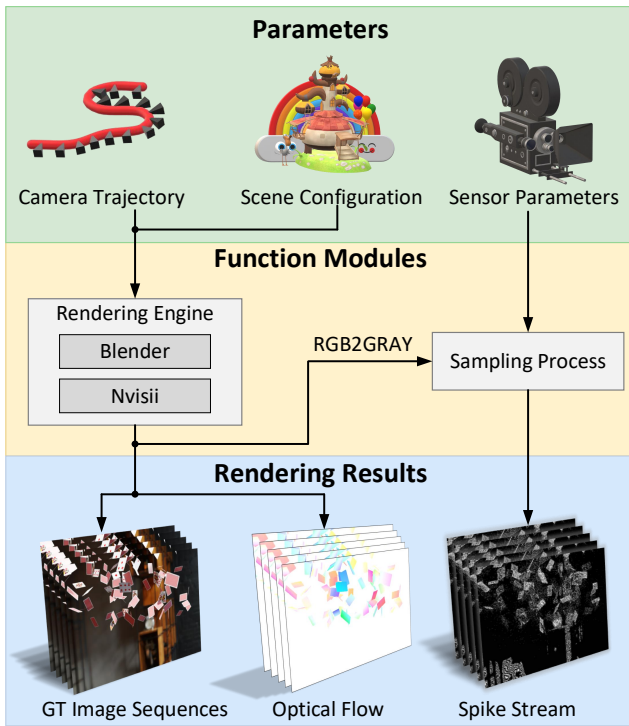


Figure 4: The framework of spiking camera simulator, SPCS. SPCS relies on a tight coupling with the rendering engine to generate spike stream accurately.

tween times t_i and t_j . Given a series of recorded binary spike stream $\{S_n\}$, $n = 1, 2, \dots, N$ from start to end of sampling, the goal of spiking camera optical flow estimation is to predict the optical flow F_{t_i, t_j} based on the spike stream.

Challenges Supervised learning algorithms are very powerful in optical flow estimation (Dosovitskiy et al. 2015; Sun et al. 2018). However, at present, there is no proper dataset providing both spike streams and their corresponding optical flow ground truth. Besides, image-based and event-based (Zhu et al. 2018b; Lee et al. 2020) networks are not specially designed for spike streams due to the difference of their data representation. A simple way is to input the spike stream $\{S_n\}$ between times t_i and t_j as a spike sequence for estimating W_{t_i, t_j} . Unfortunately, in this way, the length of $\{S_n\}$ increases with the increasing time interval $t_j - t_i$ which is inconvenient as the input of network. To avoid dynamic length of the input, inspired by (3), we can use spike number frame at time t as the representation of spike stream at time t where each pixel records spike numbers in a fixed temporal window across time t . Further, we only need to input two spike number frames at time t_i and t_j to a network. However, the spike numbers in a temporal window corresponds to the average brightness during this period (as (3)). When there is a lot of motion in scenes, the average brightness in the temporal window described by (3) can not accurately describe the instantaneous feature of spike stream, i.e., motion blur would be introduced to the representation.

Method

Simulator for spiking camera

Dataset is particularly important for learning-based algorithm and greatly affects the network performance. However, it is difficult to directly to obtain the optical flow in the real world accurately. Therefore, rendering provide a promising alternative to generate optical flow datasets for spiking camera. To this end, we proposed a simulator for spiking camera (SPCS) which models the analogue circuit of spiking camera. As fig.4, the architecture of SPCS mainly consists of Sensor Trajectory, Rendering Engine and Sampling process.

Sensor Trajectory : The sensor trajectory describes the motion of a sensor (virtual camera). We use the spline fitted by random points as sensor trajectory by default. Besides, we also provide other kinds of sensor trajectory.

Rendering Engine : The rendering engine can be used to generate the image sequences sampled by virtual camera in the scene. Note that we use nvisii (Nathan et al. 2020) and blender (Community 2018) as our engine.

Sampling process : The sampling process includes the interaction between rendering engine and the simulation of spiking camera, In more detail, the module first sends the Sensor Trajectory to Rendering Engine and converts them into spike stream after the virtual images are generated. Moreover, to better simulate the real situation, we also consider the influence of noise on spiking camera. Related details is in appendix.

SCFlow

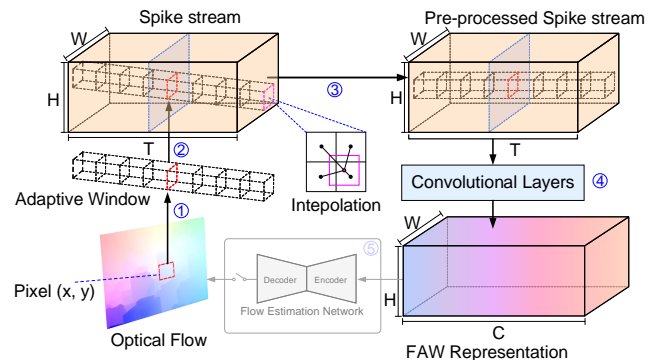


Figure 5: The architecture of proposed image-based representation of spike stream, FAW. Spike stream includes T spike frames and each spike frame corresponds to a $H \times W$ binary array. The dimension of obtained FAW is $H \times W \times C$.

Spike Stream Representation An appropriate input representation of spike stream for neural networks is crucial. Although, for each pixel, we can use the spike numbers in a fixed temporal window as the feature of spike stream at time t and input the spike number frame to network, the spike numbers express the average brightness on the same pixel over a period of time (as (3)). When there is the relative motion between the objects and the spiking camera, the

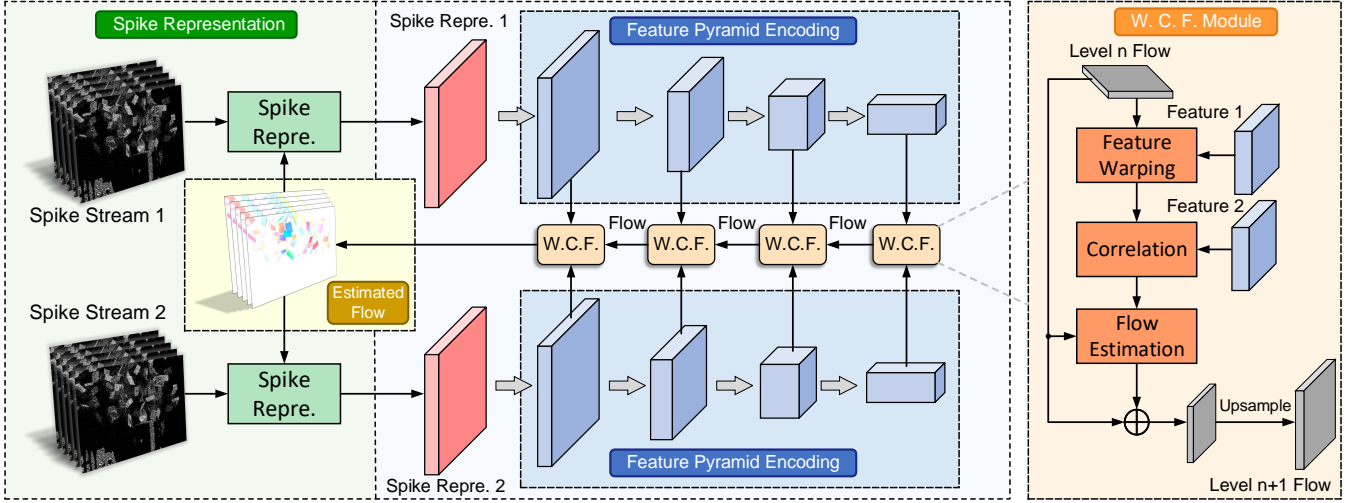


Figure 6: Network architecture of SCFlow. The spike stream is firstly represented by FAW and then constructed to be a feature pyramid. The flow is estimated through the pyramid in a coarse-to-fine manner.

brightness on the same pixel is not constant. Hence, the average brightness can not accurately describe the information of spike stream at time t , i.e., motion blur would be introduced. In order to reduce the influence of motion blur on representation at time t , selected temporal windows should be dynamic and directed. Specifically, if the direction of a temporal window is consistent with the motion trajectory of the pixel, the average brightness in the temporal window would be closer to the brightness of the pixel at time t . To this end, we introduce a proper image-based representation of spike stream, Flow-guided Adaptive Window (FAW), where the prior optical flow is used as guidance to adaptively adjust the direction of temporal windows for each pixel. For computing FAW in time t_1 , we firstly use prior optical flow in time t_1 to define the direction of temporal windows for each pixel. Specifically, the motion of pixels can be obtained from prior optical flow. Furthermore, we assume that the motion of pixels is a uniform linear motion in a very short time. Hence, the adaptive temporal window of each pixel in time t_1 is straight (as fig.5②), and for the pixel $\mathbf{x} = (x, y)$, the spike information at time t in its adaptive temporal window can be defined as

$$\mathbf{S}_{t_1}^{\text{pre}}(\mathbf{x}, t) = \mathbf{S}\left(\mathbf{x} + \frac{(t - t_1) \cdot \mathbf{W}_{t_1, t_2}(\mathbf{x})}{t_2 - t_1}, t\right), \quad (4)$$

where $t \in [t_1 - \frac{T_{\max}-1}{2}, t_1 + \frac{T_{\max}-1}{2}]$, and $\mathbf{S}_{t_1}^{\text{pre}}$ is the pre-processed spike stream recording the spike information in all adaptive temporal windows, and T_{\max} is the window length of the input spike stream. \mathbf{W}_{t_1, t_2} denotes optical flow from time t_1 to time t_2 . Note that spatial locations of the grids in adaptive temporal windows in time t may not be integer, we use the bilinear interpolated spike information in the grids (as fig.5③). Further, pre-processed spike stream at time t_1 would be encoding into a feature map with multi-channel $\mathbf{S}_{t_1}^{\text{FAW}}$ as the FAW at time t_1 by two convolutional layers with 32 channels. When estimating $\mathbf{W}_{t_1, t_2}(\mathbf{x})$, we only need

to input the FAW pair in time t_1 and time t_2 to our network. However, when computing the FAW at time t_2 , the key frame $\mathbf{S}(x, t_2)$ and flow \mathbf{W}_{t_1, t_2} are on different coordinates. According to the uniform linear motion assumption for the motion field, we implement coordinates transformation for flow to make it aligned with spike stream at time t_2 using the motion field at time t_1 (i.e. \mathbf{W}_{t_1, t_2} itself):

$$\mathcal{C}(\mathbf{W}_{t_1, t_2}(\mathbf{x})) = \mathbf{W}_{t_1, t_2}(\mathbf{x} - \mathbf{W}_{t_1, t_2}(\mathbf{x})), \quad (5)$$

$$\mathbf{S}_{t_2}^{\text{pre}}(\mathbf{x}, t) = \mathbf{S}\left(\mathbf{x} + \frac{(t - t_2) \cdot \mathcal{C}(\mathbf{W}_{t_1, t_2}(\mathbf{x}))}{t_2 - t_1}, t\right), \quad (6)$$

where $t \in [t_2 - \frac{T_{\max}-1}{2}, t_2 + \frac{T_{\max}-1}{2}]$, and $\mathcal{C}(\cdot)$ is the coordinate transformation operator.

In addition, there is also a key problem, *how to obtain prior optical flow* \mathbf{W}_{t_1, t_2} ? As fig.5⑤, we can use the estimation of optical flow $\hat{\mathbf{W}}_{t_1, t_2}$ as prior. Specifically, during training, we first set prior optical flow as zero matrix and a predicted optical flow can be obtained by the forward propagation of SCFlow. Then, we use the predicted optical flow as a prior to train SCFlow. During testing, the optical flows that need to be predicted is sorted in chronological order i.e., $\{\mathbf{W}_{n, n+dt}\}, n = 1, 2, \dots, N$. Due to high similarity of motion in adjacent time, the last predicted optical flow is used as a prior for the current testing i.e., the prior optical flow for estimating $\mathbf{W}_{i, i+dt}$ is $\hat{\mathbf{W}}_{i-1, i-1+dt}$.

Network Architecture The SCFlow network is designed in a pyramidal encoder-decoder manner. The inputs of the network are the FAW pairs. For each FAW, we build a 4-level feature pyramid $\{F_i^l(\mathbf{x})\}_{l=1}^4, i = 1, 2$, which denotes the feature for describing the scene at time t_i at l -th level. The feature pyramid has 32, 64, 96 and 128 channels in each level respectively.

We estimate the optical flow from higher level to lower level in pyramid. We refer to the well-known PWC-Net (Sun

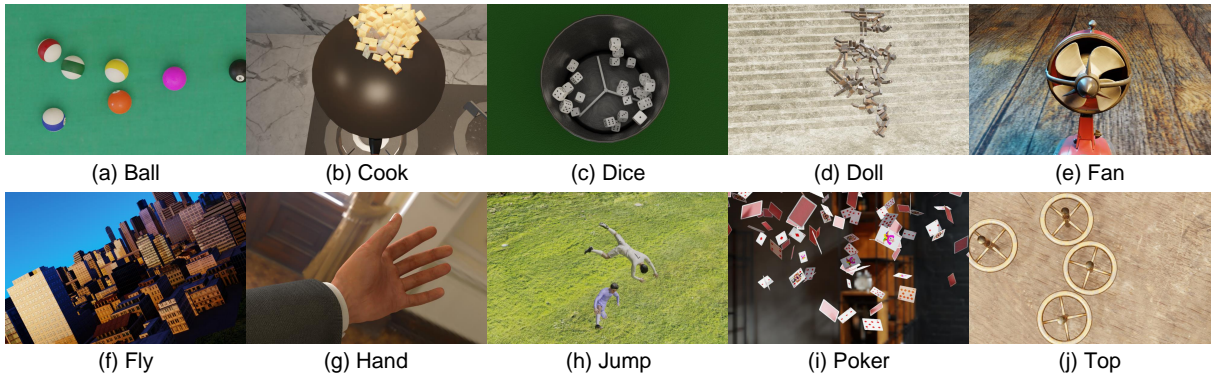


Figure 7: Scenes of Photo-realistic High-speed Motion dataset, denoted as PHM.

et al. 2018) to design the decoder. At l -th level, we firstly warp $F_2^l(\mathbf{S})$ via the current estimated flow $\hat{\mathbf{W}}_{t_1, t_2}^{l+1}(\mathbf{S})$:

$$F_{2, \hat{\mathbf{W}}_{t_1, t_2}^l}^l(\mathbf{x}) = F_2^l(\mathbf{x} + \hat{\mathbf{W}}_{t_1, t_2}^{l+1}(\mathbf{x})), \quad (7)$$

where we use bilinear interpolation for the warping operation. We use the features to build a correlation volume (Scharstein and Szeliski 2002; Xu, Ranftl, and Koltun 2017) to describe the similarity between the features. The correlation volume represents the potential displacements between the two frames, and we normalize the feature in each channel, which can be formulated as:

$$\mathbf{C}^l(\mathbf{x}, \mathbf{m}) = \left\langle \frac{F_1^l(\mathbf{x}) - \mu_1^l}{\sigma_1^l}, \frac{F_{2w}^l(\mathbf{x} + \mathbf{m}) - \mu_{2w}^l}{\sigma_{2w}^l} \right\rangle, \quad (8)$$

where \mathbf{m} represents the displacement between the two features, and $\langle \cdot \rangle$ is the inner product on channel dimension. μ and σ is the mean and standard deviation value corresponding to feature with the same subscript.

The correlation and feature 1 at current level is input to the weight-shared flow estimator. An 1×1 convolution is employed to adjust the channel numbers at different levels to be 32. The flow estimator consisting of cascaded convolutional layers predicts the residual flow. The refined flow is then upsampled via bilinear kernel as the final output of current level. The flow is supervised by its ground truth at each level:

$$\mathcal{L} = \sum_{l=1}^4 \frac{HW}{2^{4-l}} \left\| \hat{\mathbf{W}}_{t_1, t_2}^l - \mathbf{W}_{t_1, t_2}^{l, \text{gt}} \right\|_2^2, \quad (9)$$

where \mathcal{L} is our loss function, and $\mathbf{W}_{t_1, t_2}^{l, \text{gt}}$ is the ground truth of the flow at l -th level.

Experiments

Dataset

To make SCFlow learn the ability to extract an optical flow from spike streams effectively, large optical flow datasets (SPIFT and PHM) for spiking camera is firstly generated by our proposed simulator. SPIFT and PHM include 110 scenes and 10 scenes, respectively. In this study, we regard SPIFT as the training and validation set. PHM is set as the test set.

Table 1: Detailed information of datasets.

Dataset	Category	Frame	Flow density
SPIFT-Train	100	50000	100%
SPIFT-Validation	10	5000	100%
PHM-Test	10	25100	100%

There are gaps between the description of the two datasets which is beneficial to evaluate the generalization of SCFlow. The details are shown in Table 1.

SPIFT Dataset Each scene in the training set describes that different kinds of objects translate and rotate in random background (fig.2), like FlyingChairs (Dosovitskiy et al. 2015), and includes spike streams with 500 frames, corresponding GT images and optical flow. We generate optical flow every 10 spike frames ($dt=10$) and 20 spike frames ($dt=20$) separately because the motion of objects is extremely small at each spike frame timestamp (40000Hz). all parameters for scenes (number of objects, size and initial positions of objects, transformation of objects) are randomly set to improve generalization. Additional details is in appendix.

PHM Dataset Each scene in the testing set is carefully designed and has a lot in common with the real world. As shown in fig.7, “Ball” describes that billiard balls collide with each other. “Cook” describes that the vegetables are stirred in a pot. “Dice” describes the rotation of dice. “Doll” describes that some dolls fall from high onto the steps. “Fan” describes fan blade rotation of electric fan. “Fly” describes that the Unmanned Aerial Vehicle aerial scene. “Hand” describes that an arm waves in front of the moving camera. “Jump” describes that two people tumble and jump. “Poker” describes that pokers are thrown into the air. “Top” describes that the four tops spin fast and collides.

Implementation Details

We train our end-to-end model on the training set of SPIFT in PyTorch. All models are trained by Adam optimizer with $\beta_1 = 0.9$ and $\beta_2 = 0.99$. We set the learning rate as $1e-4$.

Table 2: Average end point error comparison with other methods for estimating optical flow on PHM datasets under dt=10 and dt=20 settings. The best results for each scene and the best average results are marked in bold.

	Method	Param.	Ball	Cook	Dice	Doll	Fan	Fly	Hand	Jump	Poker	Top	AVG.
dt=10	EV-FlowNet	53.43M	0.571	3.000	0.761	1.273	0.928	11.599	5.011	0.742	1.167	2.762	3.590
	Spike-FlowNet	13.04M	0.482	3.509	0.568	0.786	0.901	12.003	4.898	0.780	0.693	2.617	3.577
	SCFlow-w/oR	0.57M	0.614	1.989	1.303	0.514	0.409	9.715	2.294	0.268	1.131	2.474	2.809
	SCFlow (ours)	0.80M	0.632	1.620	1.224	0.259	0.293	9.418	1.811	0.130	0.943	2.171	2.568
dt=20	EV-FlowNet	53.43M	1.151	5.637	1.927	1.821	1.854	22.828	9.608	0.827	2.522	5.316	6.980
	Spike-FlowNet	13.04M	0.987	7.048	1.122	3.039	1.839	25.130	9.816	1.902	1.397	5.423	7.565
	SCFlow-w/oR	0.57M	1.361	3.654	2.924	1.285	0.811	20.729	4.460	0.447	2.158	4.609	5.844
	SCFlow (ours)	0.80M	1.115	3.320	2.582	0.515	0.566	20.835	4.442	0.240	1.884	4.301	5.583

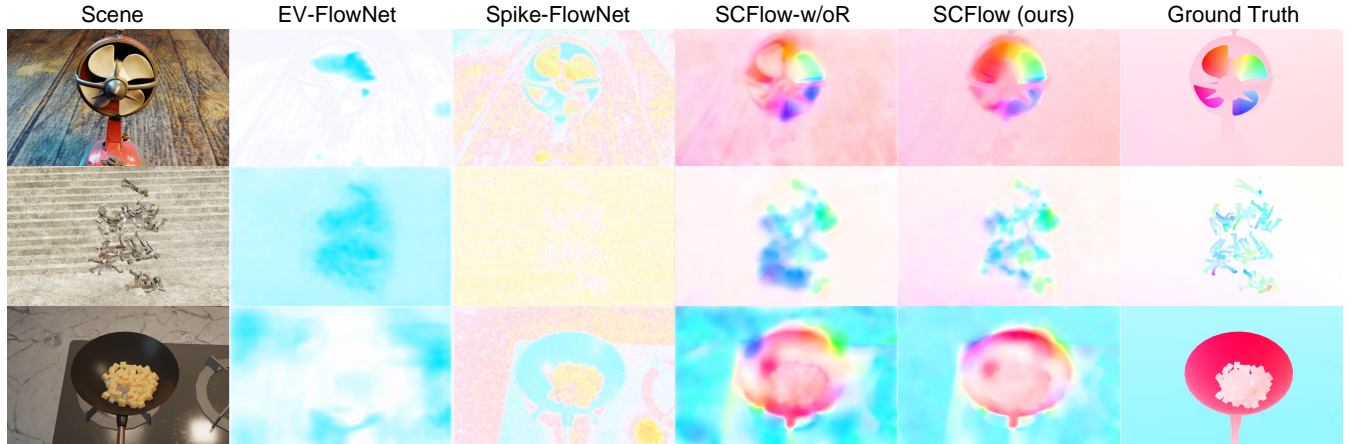


Figure 8: Visual comparison of our SCFlow with other method. The explanations of each columns of images are at the top.

and train 40 epochs for “dt=10” model and 80 epochs for “dt=20” model. We keep the input from SPIFT as the original 500×800 resolution. The batch size in training is set as 4, and we train our models on NVIDIA Tesla A100s.

Comparison Results

We compare our method with two categories of methods:

Neural network without spike representation methods. We compare our method with SCFlow network without FAW representation (SCFlow-w/oR).

Neural network in event-based optical flow with a representation method in event-based way. We compare our network with classical EV-FlowNet (Zhu et al. 2018b) and Spike-FlowNet (Lee et al. 2020), which are retrained in the same way with SCFlow. The Spike-FlowNet estimates optical flow in a recurrent manner, we split our spike streams to slices with length equals to 2.

We use average end point error (AEPE) as the evaluation metric, which indicates the average ℓ_2 norm of the error motion vector between predicted flow and its ground truth. The quantitative comparison results are shown in Table 2. In both “dt=10” and “dt=20” settings, our SCFlow gets the best average performance in all methods with a lot fewer parameters. The comparison between SCFlow-w/oR and SCFlow demonstrates that our proposed spike representation FAW can improve the accuracy of optical flow esti-

mation, which can be viewed as the ablation experiments for FAW. The visualization results are shown in fig.8. Evidently, the EV-FlowNet and Spike-FlowNet cannot estimate optical flow of spiking camera well, which demonstrates the information processing pattern are not appropriate for spiking stream. The flow visualization of SCFlow includes finer motion boundaries and textures than SCFlow-w/oR, which demonstrates the efficiency of the FAW representation.

Conclusion

In this paper, we present, SCFlow, the first novel deep learning pipeline for optical flow estimation for spiking camera. To input spike stream into our network easily, an proper input representation of spike stream, FAW, is designed where the predicted optical flow is used as an auxiliary to avoid undesired motion blur. Further, to train SCFlow, we propose the first spiking camera simulator, SPCS and, by using SPCS to render virtual scenes, the optical flow datasets (SPIFT and PHM) for spiking camera are generated first. Finally, we show that the SCFlow can predict optical flow from spike stream in different high-speed scenes, and express superiority to existing methods on the datasets. All codes and constructed datasets will be publicly available.

References

- Baker, S.; Scharstein, D.; Lewis, J.; Roth, S.; Black, M. J.; and Szeliski, R. 2011. A database and evaluation methodology for optical flow. *International Journal of Computer Vision (IJCV)*, 92(1): 1–31.
- Bideau, P.; RoyChowdhury, A.; Menon, R. R.; and Learned-Miller, E. 2018. The best of both worlds: Combining cnns and geometric constraints for hierarchical motion segmentation. In *IEEE Conference on Computer Vision and Pattern Recognition (CVPR)*, 508–517.
- Brox, T.; Bruhn, A.; Papenber, N.; and Weickert, J. 2004. High accuracy optical flow estimation based on a theory for warping. In *European Conference on Computer Vision (ECCV)*, 25–36.
- Butler, D. J.; Wulff, J.; Stanley, G. B.; and Black, M. J. 2012. A naturalistic open source movie for optical flow evaluation. In *European Conference on Computer Vision (ECCV)*, 611–625.
- Christian, B.; and Raphael, B. 2014. A 240×180 130 db 3 μ s latency global shutter spatiotemporal vision sensor. *IEEE Journal of Solid-State Circuits (JSSC)*, 49(10): 2333–2341.
- Christoph, P.; Daniel, M.; and Rainer, W. 2008. An asynchronous time-based image sensor. *IEEE International Symposium on Circuits and Systems (ISCAS)*, 49(10): 2130–2133.
- Community. 2018. Blender - a 3D modelling and rendering package. <http://www.blender.org>.
- Ding, Z.; Zhao, R.; Zhang, J.; Gao, T.; Xiong, R.; Yu, Z.; and Huang, T. 2021. Spatio-Temporal Recurrent Networks for Event-Based Optical Flow Estimation. *arXiv preprint arXiv:2109.04871*.
- Dong, S.; Zhu, L.; Tian, Y.; and Huang, T. 2017. An efficient coding method for spike camera using inter-spike intervals. In *Data Compression Conference (DCC)*, 437–437.
- Dosovitskiy, A.; Fischer, P.; Ilg, E.; Hausser, P.; Hazirbas, C.; Golkov, V.; Van Der Smagt, P.; Cremers, D.; and Brox, T. 2015. FlowNet: Learning optical flow with convolutional networks. In *IEEE International Conference on Computer Vision (ICCV)*, 2758–2766.
- Geiger, A.; Lenz, P.; and Urtasun, R. 2012. Are we ready for autonomous driving? the kitti vision benchmark suite. In *IEEE Conference on Computer Vision and Pattern Recognition (CVPR)*, 3354–3361.
- Guo, M.; Huang, J.; and Chen, S. 2017. Live demonstration: A 768×640 pixels 200meps dynamic vision sensor. *IEEE International Symposium on Circuits and Systems (ISCAS)*, 1–1.
- Horn, B. K.; and Schunck, B. G. 1981. Determining optical flow. *Artificial Intelligence (AI)*, 17(1-3): 185–203.
- Ilg, E.; Mayer, N.; Saikia, T.; Keuper, M.; Dosovitskiy, A.; and Brox, T. 2017. FlowNet 2.0: Evolution of optical flow estimation with deep networks. In *IEEE Conference on Computer Vision and Pattern Recognition (CVPR)*, 2462–2470.
- Jason, J. Y.; Harley, A. W.; and Derpanis, K. G. 2016. Back to basics: Unsupervised learning of optical flow via brightness constancy and motion smoothness. In *European Conference on Computer Vision (ECCV)*, 3–10.
- Lee, C.; Kosta, A. K.; Zhu, A. Z.; Chaney, K.; Daniilidis, K.; and Roy, K. 2020. Spike-FlowNet: event-based optical flow estimation with energy-efficient hybrid neural networks. In *European Conference on Computer Vision (ECCV)*, 366–382.
- Liu, L.; Zhang, J.; He, R.; Liu, Y.; Wang, Y.; Tai, Y.; Luo, D.; Wang, C.; Li, J.; and Huang, F. 2020. Learning by analogy: Reliable supervision from transformations for unsupervised optical flow estimation. In *IEEE Conference on Computer Vision and Pattern Recognition (CVPR)*, 6489–6498.
- Liu, P.; Lyu, M.; King, I.; and Xu, J. 2019. SelfFlow: Self-supervised learning of optical flow. In *IEEE Conference on Computer Vision and Pattern Recognition (CVPR)*, 4571–4580.
- Meister, S.; Hur, J.; and Roth, S. 2018. UnFlow: Unsupervised learning of optical flow with a bidirectional census loss. In *AAAI Conference on Artificial Intelligence (AAAI)*.
- Menze, M.; and Geiger, A. 2015. Object scene flow for autonomous vehicles. In *Proceedings of the IEEE Conference on Computer Vision and Pattern Recognition (CVPR)*, 3061–3070.
- Nathan, M.; Jonathan, T.; Stan, B.; and Ingo, W. 2020. NVISII: NVIDIA Scene Imaging Interface. <https://github.com/owl-project/NVISII>.
- Patrick, L.; Christoph, P.; and Tobi, D. 2008. A 128×128 120 db 15 μ s latency asynchronous temporal contrast vision sensor. *IEEE Journal of Solid-State Circuits (JSSC)*, 43(2): 566–576.
- Scharstein, D.; and Szeliski, R. 2002. A taxonomy and evaluation of dense two-frame stereo correspondence algorithms. *International Journal of Computer Vision (IJCV)*, 47(1): 7–42.
- Sun, D.; Roth, S.; and Black, M. J. 2010. Secrets of optical flow estimation and their principles. In *IEEE Conference on Computer Vision and Pattern Recognition (CVPR)*, 2432–2439.
- Sun, D.; Yang, X.; Liu, M.-Y.; and Kautz, J. 2018. Pwc-net: Cnns for optical flow using pyramid, warping, and cost volume. In *IEEE Conference on Computer Vision and Pattern Recognition (CVPR)*, 8934–8943.
- Tobi, D.; and Bernabe, L. 2010. Activity-driven, event-based vision sensors. *IEEE International Symposium on Circuits and Systems (ISCAS)*, 2426–2429.
- Tu, Z.; Li, H.; Zhang, D.; Dauwels, J.; Li, B.; and Yuan, J. 2019. Action-stage emphasized spatiotemporal VLAD for video action recognition. *IEEE Transactions on Image Processing (TIP)*, 28(6): 2799–2812.
- Wang, L.; Guo, Y.; Liu, L.; Lin, Z.; Deng, X.; and An, W. 2020. Deep video super-resolution using HR optical flow estimation. *IEEE Transactions on Image Processing (TIP)*, 29: 4323–4336.
- Xu, J.; Ranftl, R.; and Koltun, V. 2017. Accurate optical flow via direct cost volume processing. In *Proceedings of the IEEE Conference on Computer Vision and Pattern Recognition (CVPR)*, 1289–1297.

- Zhao, J.; Xiong, R.; and Huang, T. 2020. High-Speed Motion Scene Reconstruction for Spike Camera via Motion Aligned Filtering. In *International Symposium on Circuits and Systems (ISCAS)*, 1–5.
- Zhao, J.; Xiong, R.; Liu, H.; Zhang, J.; and Huang, T. 2021. Spk2ImgNet: Learning to Reconstruct Dynamic Scene from Continuous Spike Stream. In *IEEE Conference on Computer Vision and Pattern Recognition (CVPR)*, 11996–12005.
- Zheng, Y.; Zheng, L.; Yu, Z.; Shi, B.; Tian, Y.; and Huang, T. 2021. High-speed Image Reconstruction through Short-term Plasticity for Spiking Cameras. In *IEEE Conference on Computer Vision and Pattern Recognition (CVPR)*, 6358–6367.
- Zhu, A. Z.; Thakur, D.; Özaslan, T.; Pfrommer, B.; Kumar, V.; and Daniilidis, K. 2018a. The multivehicle stereo event camera dataset: An event camera dataset for 3D perception. *IEEE Robotics and Automation Letters*, 3(3): 2032–2039.
- Zhu, A. Z.; Yuan, L.; Chaney, K.; and Daniilidis, K. 2018b. EV-FlowNet: Self-supervised optical flow estimation for event-based cameras. *arXiv preprint arXiv:1802.06898*.
- Zhu, A. Z.; Yuan, L.; Chaney, K.; and Daniilidis, K. 2019a. Unsupervised event-based learning of optical flow, depth, and egomotion. In *IEEE Conference on Computer Vision and Pattern Recognition (CVPR)*, 989–997.
- Zhu, L.; Dong, S.; Huang, T.; and Tian, Y. 2019b. A retina-inspired sampling method for visual texture reconstruction. In *IEEE International Conference on Multimedia and Expo (ICME)*, 1432–1437.
- Zhu, L.; Dong, S.; Li, J.; Huang, T.; and Tian, Y. 2020. Retina-like Visual Image Reconstruction via Spiking Neural Model. In *IEEE Conference on Computer Vision and Pattern Recognition (CVPR)*, 1435–1443.